

# Impact of sea-ice cover on storm-mediated atmospheric warming over the Barents Sea: A regional modelling study

Atsuyoshi MANDA<sup>1</sup>

<sup>1</sup>*Graduate School of Bioresources, Mie University, Tsu, Japan*

(Received October 31, 2020; Revised manuscript accepted January 13, 2021)

## Abstract

Sea-ice loss is believed to be one of the key processes in the recent Arctic warming. This study examines the impact of sea-ice cover on the atmospheric warming associated with cyclones. Although cyclones are an important component in the Arctic climate system, details regarding the process of heat transfer during life cycles of cyclones remain unclear. The cyclone that occurred over the Barents Sea in January 21–25, 2011 was selected as the test case given that it was well validated using in-situ data. The results of numerical simulations showed that the changes in surface heat fluxes and net long-wave radiation owing to sea-ice cover changes resulted in atmospheric warming via vertical diffusion, countered by cold advection within the atmospheric boundary layer, which corroborates earlier studies. The simulations also showed that sea ice decline intensified the advection of warm air over areas north of the sea-ice edge resulting from the southerlies associated with the cyclone and caused further atmospheric warming east of Svalbard. It was also observed that a large fraction of warmed air parcels traveled well above the top of the boundary layer. This enhanced “on-ice” flow regime and upglide of the warmed air parcels associated with cyclones could play a role in spreading out the effect of anomalous heat supply due to the sea-ice decline and contribute to further atmospheric warming in the Arctic during winter.

**Keywords:** cyclone; Arctic amplification; heat transport; polar WRF

## 1. Introduction

Over the past decades, rapidly enhanced atmospheric warming has been observed in the Arctic. This warming, a phenomenon known as Arctic amplification (AA), has been occurring at the Arctic at a much faster rate compared with the rest of the world, and it is more pronounced in the lower troposphere during the cold season than during other seasons. Sea-ice cover in the Arctic exhibits a continued and drastic decline (Fig. 1; Norwegian Polar Institute, 2020). Such decline in sea-ice cover affects the energy exchange between the ocean and the atmosphere, and this is a key factor associated with the accelerated warming observed in the Arctic (Screen and Simmonds, 2010; Dai and others, 2019). Particularly, significant sea-ice reduction that can influence cold winter extremes over the Eurasian continent have been observed over the Barents and Kara Seas (Inoue and others, 2012; Mori and others, 2019), and a recent study has shown that improving the accuracy of Arctic temperature forecasts offers potential for better prediction of Arctic-midlatitude teleconnection patterns as well as seasonal prediction in mid-latitudes during winter (Jung and others, 2020).

Several mechanisms, including the central role of sea-ice loss, have been proposed to explain the AA; however, their relative importance with respect to Arctic

warming is still disputed. Both recent data analysis and numerical modelling studies have emphasized the importance of surface heat fluxes in AA (Dai and others, 2019; Kim and others, 2019). One of the interesting issues here is atmospheric heat transport. During winter, vertical temperature profiles exhibit strong stable conditions with the frequent occurrence of strong inversions in the Arctic. Such atmospheric environments prohibit vertical heat transfer across the top of the boundary layer. However, inspecting only surface fluxes cannot clarify whether the intensified vertical diffusion associated with destabilization near the surface is the sole mechanism for the vertical heat transport.

It is well known that cyclones constitute an important component of the Arctic climate system (Serreze, 1995). They can also affect the concentration and melting of sea ice (Boisvert and others, 2016). Cyclone activity largely determines the variability and changes of sea ice export from the central Arctic Ocean into the Greenland–Iceland–Norwegian Sea through Fram Strait (Wei and others, 2019). This transport comprises the largest portion of the total Arctic sea ice export (Serreze and others, 2006) and plays an important role with the drastic retreat and thinning of Arctic sea ice cover in recent years (Wei and others, 2019). Small scale cyclones in the Arctic (polar lows) affect the short-term variations of

inflow of Atlantic warm water through the Fram Strait (Sun and Gao 2018).

Cyclones can intensify surface heat fluxes via stronger surface winds. Inoue and Hori (2011) and Manda and others (2020; hereinafter referred to as M20) suggested the importance of cyclones in the storm-mediated atmospheric warming in the lower troposphere, which possibly plays a role in the recent Arctic warming. However, the effect of sea-ice cover on this process has not yet been examined.

The aim of this study is to elucidate the impact of the sea-ice cover on storm-mediated atmospheric warming. A number of numerical simulations have been performed in previous studies to examine the effect of sea-ice loss on atmospheric circulation and thermodynamic fields in the Arctic (Screen and others, 2018). However, most of these studies were focused on large scale climatological fields. Details regarding the process of heat transfer during life cycles of cyclones are still unclear. This study focuses on the cyclone that was observed in January 2011 over the Barents Sea, documented in M20. The Barents Sea is one of the areas with the highest cyclone occurrence frequency in the Arctic during winter (Raible and others, 2008). Using in-situ atmospheric soundings and surface meteorological observations, this cyclone has been realistically simulated and well validated (M20). It provides assurance regarding the reliability and suitability of the simulated results for the sensitivity experiments documented in this paper.

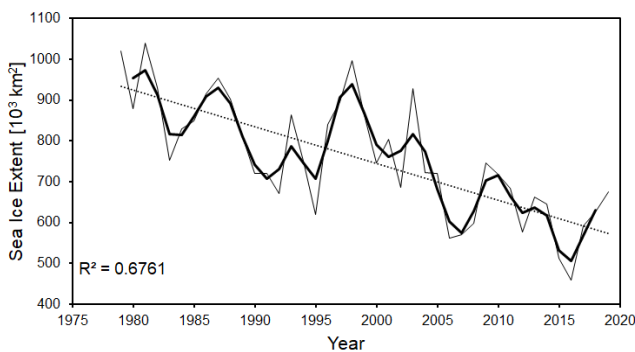


Fig. 1 Time series of changes in sea-ice extent in the Barents Sea in April, averaged over the area demarcated by latitudes 72°N and 82°N and longitudes 10°E and 60°E. The thin and thick solid lines represent monthly mean values for each year and smoothed values using the 1-2-1 filter, respectively. The dotted line represents a linear regression.

In recent studies, an increasing trend of cyclone frequency and intensity in the Arctic has been reported and a possible link with sea-ice loss has also been suggested (Rinke and others, 2017; Zahn and others, 2018; Akperov and others, 2020). The results of this study will enhance understanding regarding recent

Arctic warming, and will contribute to the projection of such warming in future.

The rest of this paper is organized as follows. The data and methods used in the study are described in Section 2, and in Section 3, the results of the numerical simulations are presented. Finally, a summary and a brief discussion are provided in Section 4.

## 2. Data and Method

### 2.1 Atmospheric model

To elucidate the effect of sea-ice cover on atmospheric warming during the life cycle of a cyclone, numerical simulations were performed. For the most part, the set-up of the model was similar to those used in M20, with some minor modifications. Details regarding the model set-up can be obtained from M20. To perform the simulations, the polar-optimized Weather Research and Forecasting model (Polar WRF; version 3.7.1) developed by Hines and Bromwich (2008) was used, rather than version 3.5.1 that was used in M20. Instead of European centre for medium-range weather forecasts interim reanalysis data (Dee and others, 2011), fifth generation atmospheric reanalysis data obtained from the European Centre for medium-range weather forecasts (ERA5; Hersbach and others, 2020) was employed for the initial and boundary conditions of the prognostic variables of the model, including sea-surface temperature (SST) and sea-ice concentrations. All other set-ups, including sub-grid scale parameterizations and model grid spacings, were the same as those in M20. Only slight differences existed between the WRF models, the atmospheric data, and the oceanic data corresponding to M20 and those corresponding to this study. We also confirmed that relative to M20, the modifications described above had little effect on the life cycle of the simulated cyclone.

### 2.2 Numerical experiments

To examine the impact of sea-ice cover on the atmospheric warming, two ensemble experiments, namely the control (CNTL) and high ice (HICE) experiments, were conducted. The CNTL experiment was carried out to reproduce the life cycle of the observed cyclone, in accordance with M20. In the HICE experiment, the set-ups employed were almost the same as those in the CNTL experiment; however, to elucidate the impact of sea-ice cover in different years, the sea-ice cover in 1981, during which the extent of the sea-ice cover was much higher than that in 2011, was utilized. All other conditions were similar to those employed in the CNTL experiment. The only difference between the CNTL and HICE experiments was sea-ice cover. To examine the sole effect of sea-ice cover, we adopted this strategy based on previous studies (Magnusdottir and others, 2004; Higgins and others, 2009; Deser and others, 2010). Behavior of cyclones can be affected by many

processes, including low-level baroclinicity, static stability (Akperov and others, 2020), and upper-level potential vorticity (PV) anomaly (M20). They can complicate the response of the simulated cyclone and may obscure the impact of the sea-ice cover.

To evaluate the uncertainty resulting from internal model variability, each ensemble experiment consisted of 23 hindcast simulations with different initial times (Bassett and others, 2020), unlike the previous modeling study (Adakudlu and Barstad, 2011). From 01 UTC January 19, 2011, time integration of each ensemble member was started at 1-h intervals until 00 UTC January 20, 2011. From this point, all the 23 members were run for a further 5-day period, ending on 00 UTC January 25, 2011. The data corresponding to the period before 00 UTC January 21, 2011 was discarded as spin up, following the strategy used in Bassett and others (2020).

### 3. Results

Figure 2 shows the tracks of the simulated cyclones, which were found to be very similar to those in M20 (Fig. 6 of M20). After initiated east of Greenland, they moved eastwards towards the sea ice edge east of Svalbard.

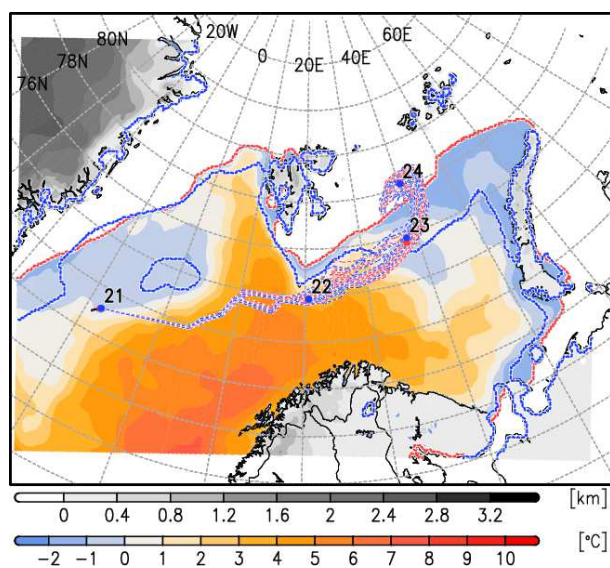


Fig. 2 Tracks of the simulated cyclones. The red and blue lines indicate the CTRL and HICE experiments, respectively. The dots indicate the location of the cyclone centers of the ensemble means at 00 UTC on the date represented by numerals. The thick dotted lines represent the sea-ice edge. Color, and black and white shades indicate SST and topography, respectively.

They were almost stationary after January 24th. The tracks in CTRL were very similar to those in HICE, indicating that differences in sea-ice cover do not have a significant impact on the track of the cyclones. This is consistent with the findings of M20, which showed that

the shutting off of surface heat fluxes changed the cyclone tracks to a limited extent. This observation is partly due to the dominance of the upper-level PV anomaly with respect to cyclone development, as shown in M20, and like in M20, the CTRL also reproduced the observed wind and temperature fields well (figure not shown).

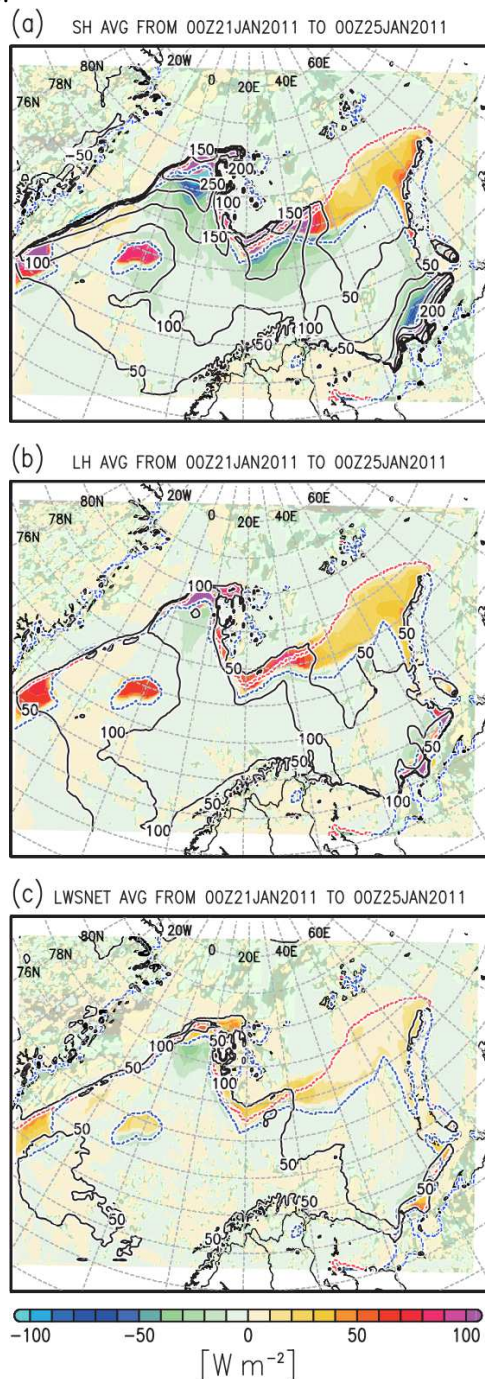


Fig. 3 Horizontal distributions of (a) SHF, (b) LHF, and (c) net LWR, averaged from 00 UTC January 21–25, 2011 (positive upward). The colors indicate differences in ensemble means between the CTRL and HICE experiments. The black contours indicate values in CTRL.

Figure 3 depicts the ensemble means of the surface heat fluxes, averaged from 00 UTC January 21–25, 2011 between the CNTL and the HICE experiments. Areas of surface heat flux change generally correspond to that of the sea ice cover. The sensible heat flux (SHF) in CNTL showed large values around the sea-ice edge west of Svalbard (Fig. 3(a)). This could be attributed to the cold air outbreak that occurred after January 22, 2011 (Fig. 5(a), M20). The latent heat flux (LHF) and net long-wave radiation (LWR) exhibited a similar tendency.

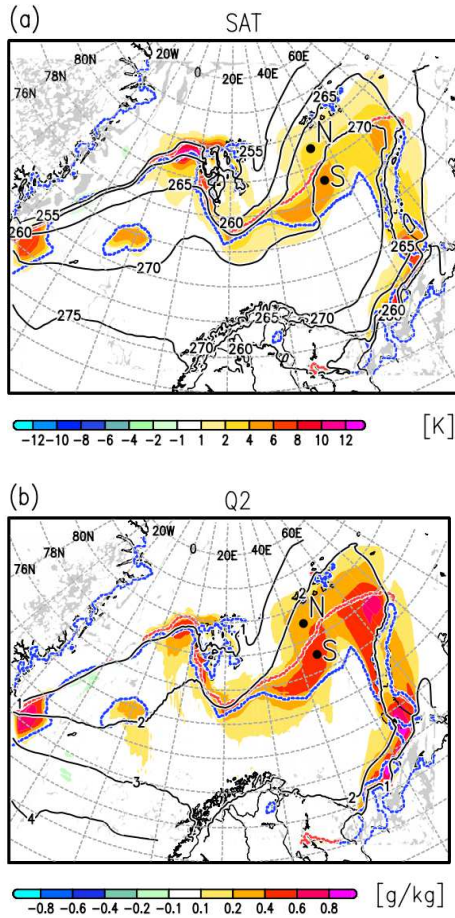


Fig. 4 Same as Fig. 3, but for (a) SAT and (b) Q2. The dots with N and S indicate the locations where the data in the time-height diagrams in Fig. 5 are sampled.

Figure 4 shows the horizontal distributions of the SAT and Q2, which is defined as the values at a height of 2 m. The areas where SAT and Q2 showed positive anomaly basically corresponded with those of the positive surface flux anomalies, e.g., the eastern coast of Greenland, an isolated sea-ice area located around 76°N, 0°E in 1981, west of Svalbard, and around the sea-ice edge from the south of Svalbard to Novaya Zemlya, suggesting the importance in local energy balance such as vertical heat transport and diabatic processes in most areas with positive SAT. On the other hand, positive

SAT and Q2 anomalies farther north of the sea-ice edge east of Svalbard were found (north of 76°N and east of 30°E). These areas were found to be covered by sea ice where the surface fluxes do not heat the atmosphere directly in both the CNTL and HICE experiments, suggesting a heating mechanism other than vertical diffusion.

As expected, these surface fluxes in CNTL were larger than those in HICE over the ice-free area in CNTL. The magnitude of the positive anomaly of the LWR was relatively small, compared with those of SHF and LHF. Some areas with negative values resulted from the gaps in the location of the local maxima in these fluxes between CNTL and HICE. For example, negative SHF anomaly on the west of Svalbard is associated with the higher surface air temperature (SAT; Fig. 4b) due to the intensified SHF in CNTL north of the negative SHF anomaly.

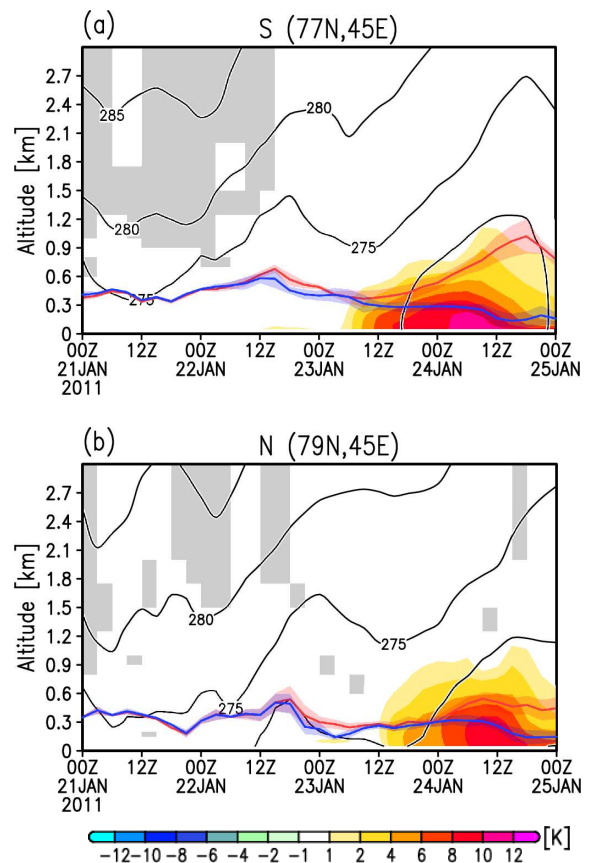


Fig. 5 Time-height diagrams of the PT in CNTL (contour) and its difference between CNTL and HICE (color) at points (a) S and (b) N shown in Fig. 4. The areas that are not gray-shaded indicate that the differences are statistically significant at a 5% confidence level. The red and blue lines indicate a boundary layer top. The transparent color shades indicate one standard deviations from the ensemble means.

Figure 5 shows the temporal evolution of the potential temperature (PT) at the points north and south of the sea-ice edge east of Svalbard, denoted “S” and “N” in Fig. 4, respectively. After 06 UTC January 23, 2011, CNTL showed higher PT in the lower troposphere at S as the boundary layer height rose. Contrarily, the boundary layer height in HICE declined gradually. On the other hand, the CNTL experiment exhibited higher PT at N after 12 UTC January 23, 2011, and the high PT anomaly appeared well above the top of the boundary layer at N, unlike the case with S. These results also indicate that the heating mechanisms at S and N are different.

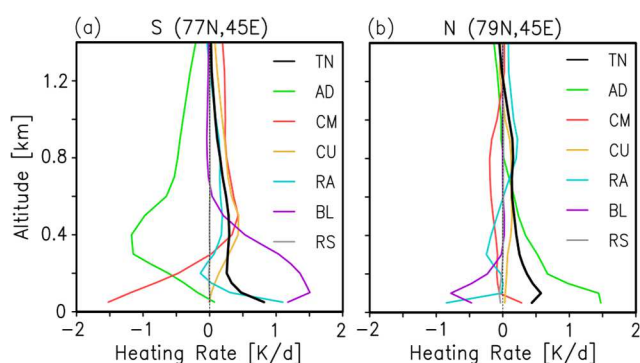


Fig. 6 Vertical profile of the difference in each term in the heat budget equation between CNTL and HICE at (a) S and (b) N, averaged within the January 23–25, 2011 period. TN represents tendency (rate of time change) of PT to change. AD, CM, CU, RA, and BL indicate heating terms due to advection, cloud microphysics, cumulus, radiation, and turbulence closure schemes, respectively. RS indicates the residual term, which is mainly due to numerical truncation errors.

Figure 6 shows the vertical profile of the difference in each term of the energy conservation (heat budget) equation between CNTL and HICE, averaged from 00 UTC January 23–25, 2011 at S and N. Positive values indicated that CNTL exhibits larger values compared with HICE. Specifically, at S, warmer air in the lower part of the troposphere was mainly caused by vertical diffusion and near surface radiation (Fig. 6(a)). The radiation term only consisted of LWR. Short-wave radiation was zero since the simulation corresponded to the polar night period. Advection counteracted this heating and cooled the air column. This advective cooling was caused by the cold air outbreak that occurred west of Svalbard and the counterclockwise circulation associated with the cyclone (Fig. 5 of M20). Near surface cooling by the cloud microphysics schemes in CNTL was presumably attributed to the upward displacement of the cloud base height associated with the destabilization of the air column. The heat balance in other areas with positive SAT anomalies was very similar to that at S, i.e., heating resulting from vertical

diffusion counteracted by horizontal advection (figure not shown).

The heating mechanism at N was different from that at S (Fig. 6(b)), and the anomalous heating of the air column was predominantly caused by advection. This advective heating was counteracted by the cooling that resulted from vertical diffusion and radiation. Their roles were found to be opposite those observed at S. After January 23, 2011, the cyclone was almost stagnant and stayed close to the sea-ice edge east of Svalbard (Fig. 1). Additionally, this cyclone caused prolonged southerlies east of the cyclone center and kept conveying warm air farther northward of the sea-ice edge (Fig. 7), where SHF and LHF were shielded and could not heat the air just above the surface. The warming process over the ice-covered area is not caused by the surface turbulent heat fluxes but by the advection term. This is a typical “on-ice” flow regime when a stable internal boundary layer develops just over the ice cover (Brümmer and Thiemann 2002; Vihma and others 2003). The southerlies in the eastern sector of the cyclone in CNTL is stronger than that of HICE (Fig. 7a), indicating that the warm advection is intensified by the anomalous winds. Serreze and others (2011) show that prominent positive temperature anomaly east of Svalbard in winter during the period of 2000–2009 corresponds to the warm advection by the anomalous wind. They also suggested the anomalous winds tend to spread out horizontally the effects of the surface heat source. The sensitivity experiment in this study reveals that the enhanced on-ice flow plays a role in spreading out the effect of intensified surface heat fluxes due to the sea-ice decline.

Figure 8 shows the forward trajectories of the air parcels released at a height of 100 m close to 76°N, 45°E. Twenty-five parcels were tracked from 00 to 12 UTC January 24, 2011 in each ensemble member. Thus, a total of 575 ( $25 \times 23$ ) parcels were used in each ensemble experiment. In both experiments, all the parcels were transported northward by the southerlies in the eastern sector of the cyclone, with slight counterclockwise turning. The latitude-height diagram showed that the air parcels in CNTL were transported further north than those in HICE (Fig. 8(b)). Additionally, the air parcels in HICE traveled at almost constant levels close to the surface without rising. The ensemble means of the height of the air parcels were well above those of the boundary layer height north of 79.6°N, and 59% of the parcels in CNTL were at least 10 m above the top of the boundary layer at 12 UTC January 24, 2011. On the other hand, only 18% of the parcels showed satisfaction with this criterion in HICE. Thus, there was a much higher chance that the air parcels heated in the boundary layer in CNTL were transported into the free troposphere, compared with those in HICE.

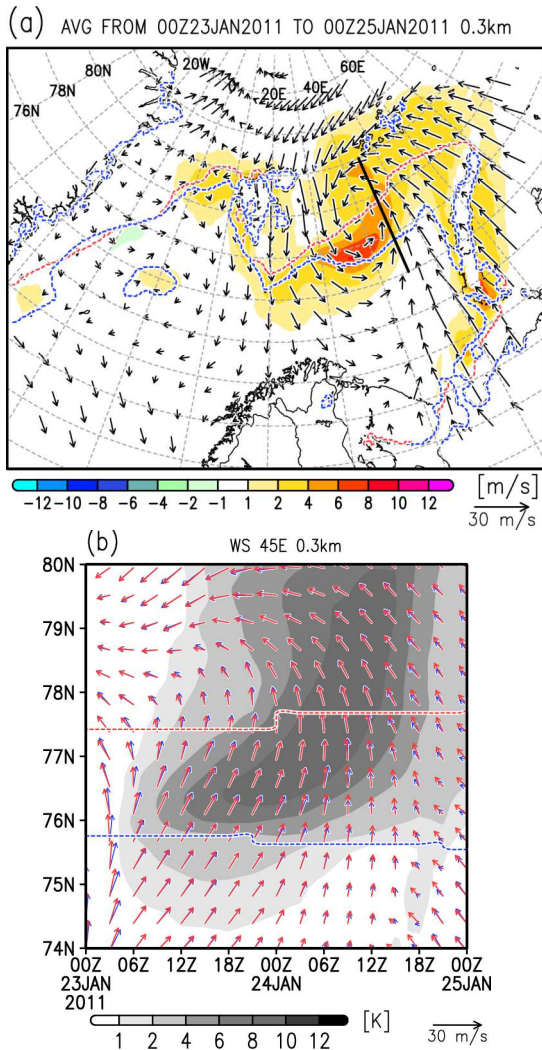


Fig. 7 (a) Horizontal wind in CNTL (vector) and difference in wind speed between CNTL and HICE (color) at a height of 300 m, averaged within the January 23–25, 2011 period. (b) Time-latitude diagram of horizontal winds and difference in PT between CNTL and HICE at a height of 300 m along the thick solid line in (a).

The static stability in the lower troposphere is very strong during winter in the Arctic. Strong inversion in the lower troposphere tended to prohibit the transportation of heat from the boundary layer to the free troposphere. Without certain atmospheric disturbances like cyclones, the possibility of transporting warmed air in the boundary layer into the free troposphere was limited. Therefore, the upglide of the warmed air due to the cyclone demonstrated in this study possibly played an important role in the anomalous heating due to the sea ice decline during winter.

#### 4. Summary and Discussion

In this study, the impact of sea-ice cover on storm-mediated atmospheric warming over the Barents Sea during winter was examined. As expected, SHF,

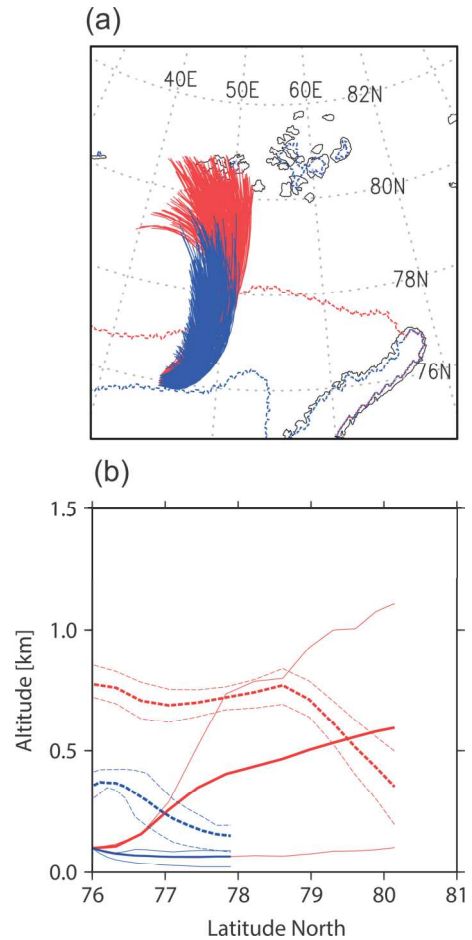


Fig. 8 (a) Forward trajectories of air parcels released at 00 UTC January 24, 2011 in the area centered at 76°N and 45°E. The dashed lines in red and blue indicate the sea-ice edge in CNTL and HICE, respectively. (b) Latitude-height diagram of the ensemble means of trajectories (thick solid lines) and boundary layer height (thick dashed lines). The thin lines indicate 25 and 75% percentiles, and the red and blue lines indicate CNTL and HICE, respectively.

LHF, and LWR in CNTL were larger than those in HICE over the area close to the sea-ice edge. These areas exhibited higher PTs within the boundary layer in CNTL than within those in HICE. The dominant mechanism that generated this temperature anomaly was anomalous heating by surface fluxes and vertical diffusion as well as radiation, counteracted by cold advection. On the other hand, the heating mechanisms farther north of the sea-ice edge east of Svalbard were quite different. The air was heated by warm advection resulting from the southerlies and cooled by vertical mixing, and in this area, anomalous heating was not limited to the boundary layer. The air parcels heated by the surface heat fluxes in CNTL traveled much higher and farther north than those in HICE. Additionally, in CNTL, there was a higher chance that the air parcels heated in the boundary layer

would be transported into the free troposphere and will travel farther north than in HICE, in which air parcels traveled at constant levels close to the surface, without rising. The strong inversions generated in the lower troposphere during winter in the Arctic prevent the air parcels from moving above the surface boundary layer, and there is little chance for the air parcels to be transported into the free troposphere in the absence of some atmospheric disturbances. This enhanced on-ice flow regime due to sea ice decline could be an important mechanism for the anomalous heating in the free troposphere in the Arctic during winter and play a role in recent Arctic warming.

The mechanism illustrated in this study is similar to that proposed by Komatsu and others (2018), who demonstrated that atmospheric warming resulting from the upglide of humid air from Siberia initiates condensational heating in a lower part of the troposphere above the boundary layer, leading to atmospheric warming in the free troposphere during summer in the Arctic. Our numerical simulations showed that condensational heating plays a secondary role in contrast to the findings of Komatsu and others (2018). Moreover, they argued that sea-ice cover is an important contributor to the upglide of humid air and heating in the atmosphere. This argument is opposite that drawn from the results of this study, which showed that a decline in sea-ice cover enhances atmospheric warming in the Barents Sea. The enhanced on-ice flow regime demonstrated in this study could play an important role in the atmospheric warming observed during winter in the Arctic, even though the sea-ice cover showed a persistent decline as is the case with the current climate.

The impact of sea-ice cover on the frequency, intensity, and track of the cyclone is still disputed (Koyama and others, 2017) given that cyclone activities in existing atmospheric reanalysis datasets are rather different (Zahn and others, 2018). However, changes in the atmospheric environment that favor cyclogenesis were surely observed in the existing datasets (Koyama and others, 2017).

This study illustrated the importance of enhanced on-ice flow regime associated with a cyclone in spreading out the effect of the anomalous heating due to the sea-ice decline during winter. Further, the results of this study provide evidence that only changes in sea-ice cover, without any other supporting mechanisms, can intensify warm advection and vertical heat transport, which was not addressed in previous studies (Higgins and Cassano, 2010; Serreze and others, 2011). Barents Sea is one of the areas of the most frequent cyclone occurrence in the Arctic during winter (e.g., Raible et al., 2009). It is also one of the key regions of the recent AA. The results of this study imply that the better representation of heat transport due to cyclones around the sea-ice edge in the climate models contributes to a

more accurate projection of future AA. A variety of cyclones occur in the Arctic and their structures and lifecycles are rather different from those of the cyclone examined in this study. Therefore, further comprehensive studies are necessary to quantify the impact of the cyclones on the Arctic climate and its change, e.g., AA.

### Acknowledgements

The author thanks K. Hines and the Polar Meteorology Group, Byrd Polar and Climate Research Center, Ohio State University for providing Polar WRF. He also thanks anonymous reviewers and Editor-In-Chief H. Kitagawa for their constructive comments. This work was supported in part by the Arctic Challenge for Sustainability II (ArCS II) Project (Program Grant Number JPMXD1420318865), the Japan Society for Promotion for Science through Grants-in-Aid for Scientific Research (Grant Numbers JP17H02958 and JP19H05697), and the Collaborative Research Program of the Research Institute for Applied Mechanics, Kyushu University (Grant Number 2020 S2-6).

### References

- Adakudlu, M. and I. Barstad (2011): Impacts of the ice-cover and sea-surface temperature on a polar low over the Nordic seas: A numerical case study. *Q.J.R. Meteorol. Soc.*, **137**: 1716–1730.
- Akperov, M., V.A. Semenov and 4 others (2020): Impact of Atlantic water inflow on winter cyclone activity in the Barents Sea: Insights from coupled regional climate model simulations. *Env. Res. Lett.*, **15**: 024009, doi:10.1088/1748-9326/ab6399.
- Bassett, R., P.J. Young and 3 others (2020): A large ensemble approach to quantifying internal model variability within the WRF numerical model. *J. Geophys. Res. Atmos.*, **125**: e2019JD031286.
- Boisvert, L.N., A.A. Petty and J.C. Stroeve (2016): The impact of the extreme winter 2015/16 Arctic cyclone on the Barents-Kara Seas. *Mon. Weather Rev.*, **144**: 4279–4287.
- Brümmer, B. and S. Thiemann (2002): The Atmospheric boundary layer in an Arctic wintertime on-ice air flow. *Boundary-Layer Meteorol.*, **104**: 53–72.
- Dai, A., D. Luo and 2 others (2019): Arctic amplification is caused by sea-ice loss under increasing CO<sub>2</sub>. *Nat. Commun.*, **10**: 121, doi:10.1038/s41467-018-07954-9.
- Dee, D.P., S.M. Uppala and 34 others (2011): The ERA-Interim reanalysis: Configuration and performance of the data assimilation system. *Q.J.R. Meteorol. Soc.*, **137**: 553–597.
- Deser, C., R. Tomas and 2 others (2010): The seasonal atmospheric response to projected Arctic sea ice loss in the late twenty-first century. *J. Clim.*, **23**: 333–351.
- Hersbach, H., B. Bell and 42 others (2020): The ERA5 global reanalysis. *Q.J.R. Meteorol. Soc.*, **146**: 1999–2049.
- Higgins, M.E. and J.J. Cassano (2010): Response of Arctic 1000 hPa circulation to changes in horizontal resolution and sea ice forcing in the Community Atmospheric Model. *J. Geophys. Res.*, **115**: D17114, doi:10.1029/2009JD013440.
- Hines, K.M. and D.H. Bromwich (2008): Development and testing of polar weather research and forecasting (WRF)

- model. Part I: Greenland ice sheet meteorology. *Mon. Weather Rev.*, **136**: 1971–1989.
- Inoue, J. and M.E. Hori (2011): Arctic cyclogenesis at the marginal ice zone: A contributory mechanism for the temperature amplification? *Geophys. Res. Lett.*, **38**: L12502, doi:10.1029/2011GL047696.
- Inoue, J., M.E. Hori and K. Takaya (2012): The role of Barents Sea ice in the wintertime cyclone track and emergence of a warm-Arctic cold-Siberian anomaly. *J. Clim.*, **25**: 2561–2568.
- Jung, E., J.-H. Jeong and 4 others (2020): Impacts of the Arctic-midlatitude teleconnection on wintertime seasonal climate forecasts. *Env. Res. Lett.*, **15**: 094045, doi:10.1088/1748-9326/aba3a3.
- Kim, K.Y., J.Y. Kim and 5 others (2019): Vertical feedback mechanism of winter Arctic amplification and sea ice loss. *Sci. Rep.*, **9**: 1184, doi:10.1038/s41598-018-38109-x.
- Komatsu, K.K., V.A. Alexeev and 2 others (2018): Poleward upgliding Siberian atmospheric rivers over sea ice heat up Arctic upper air. *Sci. Rep.*, **8**: 2872, doi:10.1038/s41598-018-21159-6.
- Koyama, T., J. Stroeve and 2 others (2017): Sea ice loss and Arctic Cyclone Activity from 1979 to 2014. *J. Climate*, **30**: 4735–4754.
- Magnusdottir, G., C. Deser and R. Saravanan (2004): The effects of North Atlantic SST and sea ice anomalies on the winter circulation in CCM3. Part I: Main features and storm-track characteristics of the response. *J. Climate*, **17**: 857–876.
- Manda, A., T. Mitsui and 4 others (2020): Storm-mediated ocean-atmosphere heat exchange over the Arctic Ocean: A case study of a Barents Sea cyclone observed in January 2011. *OSPOR*, **4**: 1–9.
- Mori, M., Y. Kosaka and 3 others (2019): A reconciled estimate of the influence of Arctic sea-ice loss on recent Eurasian cooling. *Nat. Clim. Change*, **9**: 123–129.
- Norwegian Polar Institute (2020): Sea ice extent in the Barents Sea in April. Environmental monitoring of Svalbard and Jan Mayen (MOSJ). URL: <http://www.mosj.no/en/climate/ocean/sea-ice-extent-barents-sea-fram-strait.html>.
- Raible, C.C., P.M. Della-Marta and 3 others (2008): Northern hemisphere extratropical cyclones: A comparison of detection and tracking methods and different reanalyses. *Mon. Weather Rev.*, **136**: 880–897.
- Rinke, A., M. Maturilli and 6 others (2017): Extreme cyclone events in the Arctic: Wintertime variability and trends. *Environ. Res. Lett.*, **12**: 094006, doi:10.1088/1748-9326/aa7def
- Screen, J.A., C. Deser and 10 others (2018): Consistency and discrepancy in the atmospheric response to Arctic sea-ice loss across climate models. *Nat. Geosci.*, **11**: 155–163.
- Screen, J.A., C. Deser and I. Simmonds (2012): Local and remote controls on observed Arctic warming. *Geophys. Res. Lett.*, **39**: L10709, doi: 10.1029/2012GL051598.
- Screen, J.A. and I. Simmonds (2010): The central role of diminishing sea ice in recent Arctic temperature amplification. *Nature*, **464**: 1334–1337.
- Serreze, M.C. (1995): Climatological aspects of cyclone development and decay in the Arctic. *Atmos.-Ocean*, **33**: 1–23.
- Serreze, M.C., A.P. Barrett and 8 others (2006): The large-scale freshwater cycle of the Arctic. *J. Geophys. Res.*, **111**: C11010, doi:10.1029/2005JC003424.
- Serreze, M.C., A.P. Barrett and J.J. Cassano (2011): Circulation and surface controls on the lower tropospheric air temperature field of the Arctic. *J. Geophys. Res.*, **116**: D07104, doi: 10.1029/2010JD015127.
- Sun, R. and G. Gao (2018): Impact of polar lows on synoptic scale variability of Atlantic inflow in the Fram Strait. *Acta Oceanol. Sin.* **37**: 42–50.
- Skamarock, W.C., J.B. Klemp and 7 others (2008): A description of the Advanced Research WRF version 3. *NCAR technical note NCAR/TN-475+STR*, NCAR: Boulder, CO, USA, 113pp., doi: 10.5065/D68S4MVH.
- Vihma, T., J. Hartmann and C. Lüpkes (2003): A case study of an on-ice air flow over the Arctic marginal sea-ice zone. *Boundary-Layer Meteorol.*, **107**: 189–217.
- Wei, J., X. Zhang and Z. Wang (2019): Impacts of extratropical storm tracks on Arctic sea ice export through Fram Strait. *Clim. Dyn.* **52**: 2235–2246.
- Zahn, M., M. Akperov and 3 others (2018): Trends of cyclone characteristics in the Arctic and their patterns from different reanalysis data. *J. Geophys. Res. Atmos.*, **123**: 2737–2751.

## Summary in Japanese

和文要約

### 海氷分布が低気圧を媒介とした バレンツ海の気温上昇に及ぼす影響 —領域気象モデルを用いた研究

万田敦昌<sup>1</sup>

<sup>1</sup>三重大学

海氷減少は北極温暖化の主要因と考えられているがそのメカニズムには未解明の点が多い。本研究では低気圧を媒介としたバレンツ海の昇温過程に海氷分布が及ぼす影響を、2011年1月21日から25日にかけてバレンツ海で観測された低気圧をテストケースとした数値実験によって調べた。海氷分布を変化させた領域の多くにおいて、海面熱フラックスの強化に伴って乱流鉛直拡散と長波放射が強まり、これにより大気はより加熱されていた。それとは対照的に、スピッツベルゲン島東方の海氷縁よりも極側の領域では、低気圧に伴う南風によって内部境界層がより極側に広がるとともに、暖気移流による大気加熱が強化されていた。また、海氷縁より南側の開水域で加熱された境界層内の気塊は、南風によって北上しながら境界層よりも上方の自由大気に向けて輸送されていた。冬季の北極海では逆転層を伴う強い安定成層によって、境界層と自由対流圏の熱交換が抑制されているが、本研究で示した低気圧に伴う海氷域における暖気の北上並びに上昇過程は、海氷減少に伴う冬季北極域における温暖化を促進する働きがあること示唆している。

Correspondence to: A. Manda, am@bio.mie-u.ac.jp

Copyright ©2021 The Okhotsk Sea & Polar Oceans Research Association. All rights reserved.